Nonlinear dynamics and neuronal networks : proceedings of the 63rd W.-E.-Heraeus-Seminar, Friedrichsdorf, 1990 / ed. by H. G. Schuster. – Weinheim ; New York ; Basel ; Cambridge : VCH, 1991
(Nonlinear systems ; Vol. 2)
ISBN 3-527-28342-0 (Weinheim ...) Gb.
ISBN 1-56081-167-6 (New York) Gb.

Phase Coherence and Computation in a Neural Network of Coupled Oscillators

by *H. Sompolinsky*[1], *D. Golomb,* and *D. Kleinfeld*

*** AT&T Bell Laboratories, Murray Hill, New Jersey 07974;**
† Racah Institute of Physics, Hebrew University, Jerusalem, Israel 91904.

Abstract

An oscillator neural network model that is capable of processing local and global attributes of sensory input is proposed and analyzed. Local features in the input are encoded in the average firing rate of the neurons while the relationships between these features can modulate the temporal structure of the neuronal output. Neurons that share the same receptive field interact via relatively strong feedback connections, while neurons with different fields interact via specific, relatively weak connections. The model is studied in the context of processing visual stimuli that are coded for orientation. We compare our theoretical results with recent experimental evidence on coherent oscillatory activity in the cat visual cortex. The computational capabilities of the model for performing discrimination and segmentation tasks are demonstrated. The effect of axonal propagation delays on synchronization of oscillatory activity is discussed.

Introduction

The linking of sensory inputs across multiple sensory receptive fields is a fundamental task of sensory processing. Such linkage is necessary to identify distinct objects, segment them from each other and separate them from background. The theoretical issues raised by this processing have been difficult to approach within the framework of most current neural network models. This difficulty originates from using only the levels of activity in individual neurons to encode information. It has been suggested by von der Malsburg and Schneider (1) that global properties of stimuli are identified through correlations in the temporal firing patterns of different neurons. This concept gained support from a recent series of experiments by Eckhorn and coworkers (2) and Gray and Singer and coworkers (3-6).

---

1 On leave from the Racah Institute of Physics, Hebrew University, Jerusalem, Israel 91904.

Our theoretical work is motivated by the following aspects of the experimental results on coherent oscillatory activity exhibited by neurons in the cat primary visual cortex (2-6) (Fig. 1).

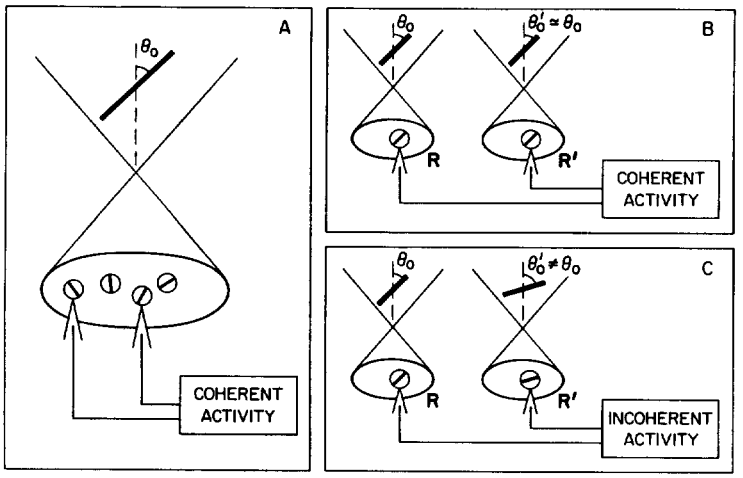

Figure 1. Schematic summary of the experimental evidence on phase between neurons in different regions of the cortex. The large ovals corresponds to the receptive field that is shared by different neurons (circles with stripes) whose individual orientation preference is indicated by the orientation of the stripe. The long bars correspond to stimuli with orientation θ_0. **A** The output of neurons that share the same receptive field are correlated, independent of their orientation preference. **B** The output of neurons in spatially separated receptive fields is correlated if the separate stimuli have the same relative orientation. **C** The output of neurons in spatially separated receptive fields is uncorrelated if the separate stimuli have the same relative orientation.

1. Neurons that respond to moving, oriented bars have a periodic component in their spiking output. The average period, $\sim$ 20 - 30 ms, appears to be the same for different neurons and is independent of the orientation of the stimulus.

2. The activity of neurons that share a receptive field can be synchronized by the presentation of a single, oriented bar. The synchronization is fairly insensitive to the orientation preferences of the neurons (Fig. 1A).

3. Neurons with separate receptive fields will fire in synchrony *only* if bars that simultaneously pass through the individual fields have similar orientation. Interestingly, this occurs even though the coherent activity of neurons that share the same receptive field is largely independent of the orientation of the stimulus (Figs. 1B and 1C).

4. The strength of the synchronization of the activity of neurons with different receptive fields is significantly enhanced by the use of a single long bar, that extends across several fields, rather than two discontinuous, short bars.

5. The outputs of neurons with different receptive fields are not synchronized if the two stimuli move in opposite directions, even for neurons that respond vigorously to both directions of motion.

6. There were no substantial phase-shifts in the temporal coherence for any of the experimental paradigms.

In this paper we describe a model neural network (7) that is capable of linking activity in disparate visual receptive fields in a manner that depends on extended features of the stimulus. The network is comprised of neurons that act as oscillators. The amplitude of their output corresponds to the average neuronal firing rate and the phase describes the temporal structure of the neuronal outputs.

The role of cortical connections in maintaining the phase coherence between neurons has been the topic of much recent investigation (8-14). Our phenomenological model of phase oscillators greatly simplifies the dynamics and permitted us to make a comprehensive, analytical treatment of the temporal and spatial coherence in terms of few parameters. Thus we were able to focus on specifying the pattern of connectivity that is capable of generating spatial and temporal coherence in neuronal output similar to that observed in experiments. Further, our model and its analysis provide explicit relations between the underlying neuronal connectivity and the capability of the network to discriminate between stimuli.

Model

Phase equations

The firing of the neurons is considered as stochastic events, described by the probability per unit time that the neuron at location $\mathbf{r}$ will fire at time t. This probability function, $P(\mathbf{r},t)$, is assumed to have the form

$$P(\mathbf{r},t) = V(\mathbf{r}) \left(1 + \lambda \cos\Phi(\mathbf{r},t)\right). \tag{1}$$

The phases $\Phi(\mathbf{r},t)$ parametrize the temporal firing pattern of the neurons. The coefficient λ corresponds to the relative contribution of the temporally modulated neuronal activity. The amplitude $V(\mathbf{r})$ is the normalized firing rate *averaged* over the duration of stimulus. If no stimulus is present within the receptive field of the neuron at $\mathbf{r}$, $V(\mathbf{r})=0$. With a stimulus moving across the field, $V(\mathbf{r})$ is taken to coincide with the 'tuning' curve of the neuron, *i.e.*,

$$V(\mathbf{r}) = V(\theta_0(\mathbf{r}) - \theta(\mathbf{r})) \tag{2}$$

where $\theta_0(\mathbf{r})$ is the orientation of the stimulus and $\theta(\mathbf{r})$ is the orientation preferred by the neuron. An illustration of a tuning curve is given in Fig. 2. We chose the form

$$V(\theta_0(\mathbf{r}) - \theta(\mathbf{r})) = e^{-|\theta_0(\mathbf{r})-\theta(\mathbf{r})|/\sigma} \tag{3}$$

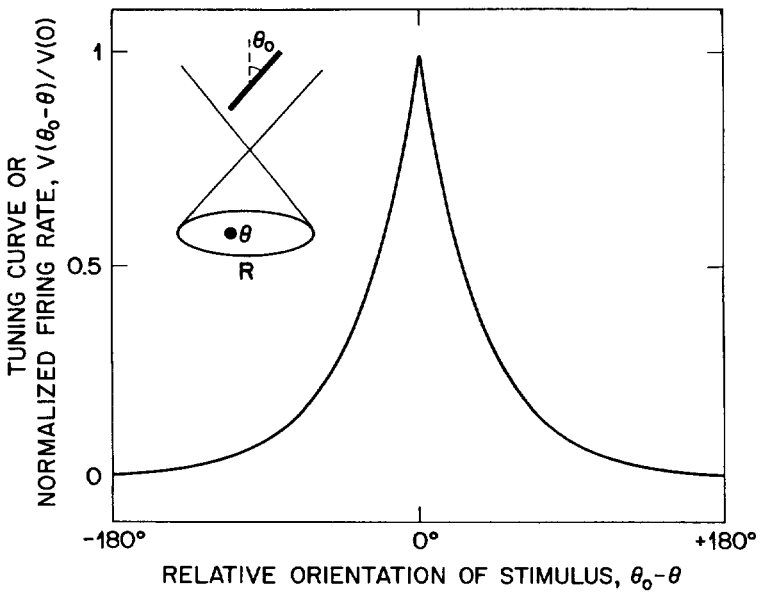

Figure 2. The tuning curve assumed for each of the neurons. The curve is the average firing rate of the neuron in response to a moving bar with orientation θ_0. The neuron has orientation preference θ. The width of the curve was taken as $\sigma = 36°$, corresponding to a half-width at half maximum of 25°(27).

where σ is the width of the tuning curve, for convenience in our analysis. Stimuli move along an axis that is perpendicular to their orientation. The difference in response to forward and reverse movement on this axis is the difference between $V(\theta)$ and $V(\theta - 180^o)$.

The phase variables that govern the temporal aspects of the neuronal activity are assumed to obey equations for a system of coupled phase-oscillators with noise (15), *i.e.*,

$$\tau_0 \dot{\Phi}(\mathbf{r},t) = \omega\tau_0 + \eta(\mathbf{r},t) - \sum_{\mathbf{r}' \neq \mathbf{r}} J(\mathbf{r}, \mathbf{r}') \sin\Big(\Phi(\mathbf{r},t) - \Phi(\mathbf{r}',t)\Big) \tag{4}$$

where τ_0 is the neuronal time-scale and ω is the frequency of the neuronal oscillations. We assume that $\tau_0 \ll 2\pi/\omega$; this is consistent with the estimates $\tau_0 \simeq 3$ ms and and $2\pi/\omega \simeq 25$ ms from experiment (2,3). The term $\eta(\mathbf{r},t)$ represents white noise with variance $<\eta(\mathbf{r},t)\,\eta(\mathbf{r}',t')> = 2T\,\tau_0\,\delta_{\mathbf{r}\mathbf{r}'}\,\delta(t-t')$, where T is a measure of the noise level. The noise represents fluctuations in the input to a cell. The connection strength $J(\mathbf{r}, \mathbf{r}')$ mediates the interaction between the phases of the neurons at locations $\mathbf{r}$ and $\mathbf{r}'$. Lastly, the sum over $\mathbf{r}'$ includes all neurons in the network.

Architecture of the connections

The interactions between the neuronal phases are assumed to encode information about the position and orientation of the stimulus. We postulate that they depend on the average level of activity of the pre- and post-synaptic cell, *i.e.*,

$$J(\mathbf{r}, \mathbf{r}') = V(\mathbf{r})\, W(\mathbf{r}, \mathbf{r}')\, V(\mathbf{r}') \tag{5}$$

where $W(\mathbf{r}, \mathbf{r}')$ specifies the architecture of the connections and is independent of the external stimulus.

A central element in this model is the introduction of short-range interactions that couple neurons with strongly overlapping receptive fields and long-range interactions that couple neurons with non-overlapping receptive fields. We assume an architecture in which neurons are grouped into clusters, analogous to hypercolumns in the primary visual cortex (16,17). The neurons in each cluster respond to a stimulus in a common receptive field. They are labeled by the spatial coordinates of the cluster, denoted **R**, and their preferred orientation, θ, which is assumed to be uniformly distributed within each cluster (Fig. 3).

Each neuron interacts with cells in the same cluster via short-range connections, taken as

$$W_{\mathrm{RR}}(\theta, \theta') = \frac{W_S}{N} \tag{6}$$

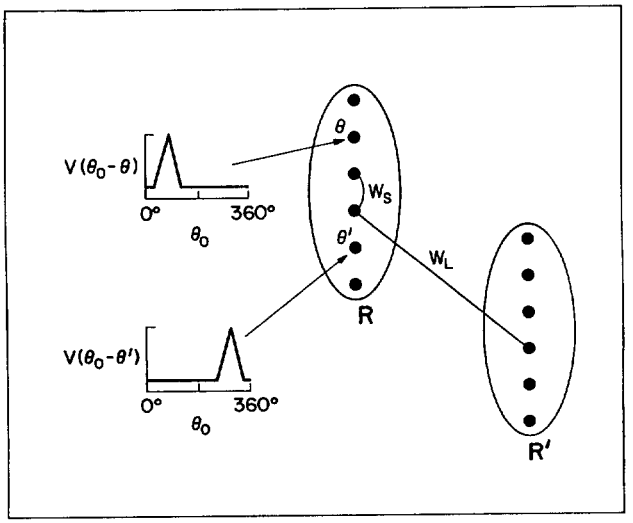

Figure 3. Schematic of the neuronal architecture assumed in our model. Neurons that share a common receptive field are grouped into clusters. Each neuron interacts with cells in the same cluster via short-range connections with strength W_S/N and with cells in different clusters via long-range connections with strength W_L/N^2.

where N is the total number of neurons in the cluster that are activated by the stimulus. The above form allows the coherence between two active neurons with the same receptive field to vary only moderately as a function of their preferred orientations. Neurons in different clusters interact via long-range connections, taken as

$$W_{\mathbf{RR}'}(\theta,\theta') = \frac{W_L}{N^2} F(\theta-\theta') ; \quad \mathbf{R}\neq\mathbf{R}' . \tag{7}$$

We have assumed that $W_{\mathbf{RR}'}(\theta,\theta')$ does not depend on the spatial separation between the clusters. The function $F(\theta-\theta')$ will be chosen, as described below, so that the phase coherence between different clusters will have a substantial dependence on the relative orientation of the stimuli. The relative strength of the long-range to the short-range connections scales as $1/N << 1$. This insures that the coherence between neurons that share the same receptive field is largely independent of the the *global* properties of the stimulus.

Feature specificity of the long-range connectivity.

Orientation selectivity. The sensitivity of the coherence between two clusters to the relative orientation of the stimuli depends on the effective interaction between the clusters. The effective interaction is related to the form of the long-range connections between neurons in the two clusters, specified by $F(\theta - \theta')$. A simplified form of the relation between $F(\theta - \theta')$ and the effective interaction, denoted $J_{\mathbf{RR}'}$, is found by averaging the interactions between all pairs of neurons in the two clusters (Eqs. 5 and 7), *i.e.*,

$$J_{\mathbf{RR}'} \simeq \frac{W_L}{N} \int_0^{2\pi} \frac{d\theta d\theta'}{\sigma^2} \; V_{\mathbf{R}}(\theta) \, F(\theta-\theta') V_{\mathbf{R}'}(\theta') \tag{8}$$

where $V_{\mathbf{R}}(\theta) \equiv V(\theta_0(\mathbf{R}) - \theta(\mathbf{R}))$. This relation is valid in the limit $W_S >> T$, for which the neurons in each cluster are fully synchronized. Note that $J_{\mathbf{RR}'}$ is a function of the difference in the orientation of the stimuli, $\Delta\theta_0 \equiv \theta_0(\mathbf{R})-\theta_0'(\mathbf{R}')$, since $V_{\mathbf{R}}(\theta)$ and $V_{\mathbf{R}'}(\theta)$ depend on the orientation of the external stimuli (Eq. 2.2).

The absence of phase-shifts in the experimentally observed cross-correlations (2,3) indicates that $J_{\mathbf{RR}'}$ is excitatory. Furthermore, experimental evidence (2,4,6) and computational considerations suggest that $J_{\mathbf{RR}'}$ is a rapidly decreasing function of $\Delta\theta_0$. To account for these properties, we consider first the possibility that the long-range connections represented by $F(\theta - \theta')$ are purely excitatory and occur only between neurons with similar orientation preferences (Fig. 4A), *i.e.*,

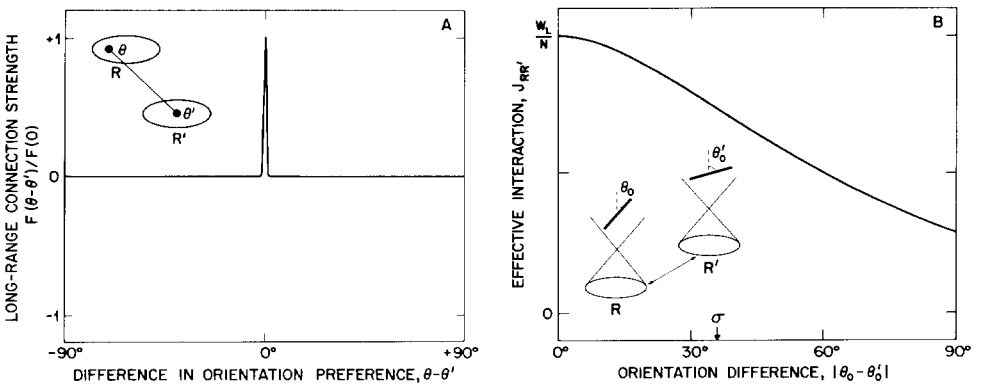

Figure 4. Interaction between two spatially separated clusters that involves purely excitatory connections. **(A)** A form for the long-range connectivity between neurons in different clusters, with orientation preferences θ and θ', in which only neurons with similar orientation preferences form excitatory connections (Eq. 9). **(B)** The effective interaction for the connectivity in part A (Eq. 10).

$$F(\theta-\theta') = \sigma\, \delta(\theta-\theta') \tag{9}$$

where $\delta(x)$ is the Dirac delta function. This hypothesis leads, for the tuning curve specified by Eq. 2.3, to

$$J_{RR'}(\Delta\theta_0) \simeq \frac{W_L}{N}\left(1 + \frac{|\Delta\theta_0|}{\sigma}\right) e^{-|\Delta\theta_0|/\sigma} . \tag{10}$$

The resultant orientation dependence is relatively weak, as shown in Fig. 4B. The angular range of this interaction is roughly twice the width of the neuronal tuning curve (Fig. 2),

Within the framework of the linear filtering (Eq. 8), a sharper dependence of $J_{RR'}$ on $\Delta\theta_0$ requires the use of inhibitory as well as excitatory long-range connections. An interesting form of such connectivity is shown in Fig. 5A, *i.e.*,

$$F(\theta - \theta') = \left(1 - \sigma^2 \frac{\partial^2}{\partial(\theta-\theta')^2}\right)^2 e^{-(\theta-\theta')^2/2\epsilon^2} \tag{11}$$

Substituting this form, together with the exponential form for the tuning curve, into Eq. 2.8 yields

$$J_{RR'}(\Delta\theta_0) \simeq \frac{W_L}{N}\, e^{-(\Delta\theta_0)^2/2\epsilon^2} \tag{12}$$

where ϵ is a free parameter that controls the angular range of the effective interaction. A reasonable choice for this parameter is $\epsilon \leq \sigma$. The results for $J_{RR'}$ with $\epsilon = 0.3\,\sigma$ are shown in Fig. 5B.

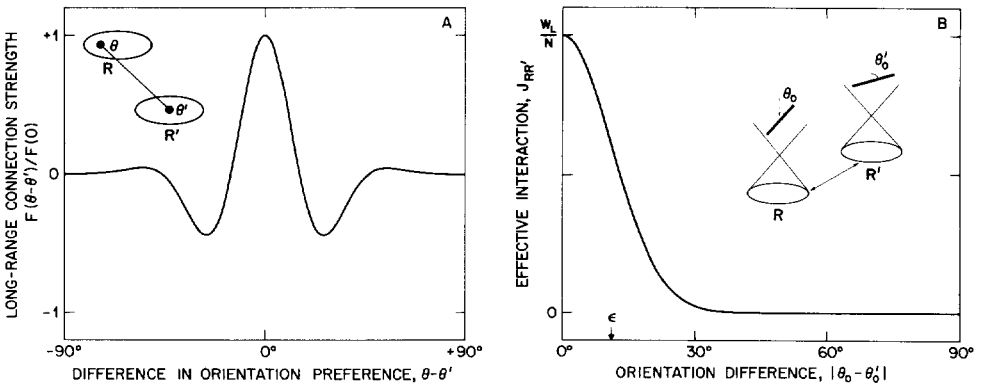

Figure 5. Interaction between two spatially separated clusters that involves both excitation and inhibition. **(A)** A form for the long-range connectivity between neurons in different clusters in which neurons with similar orientation preferences form excitatory connections and neurons with dissimilar preferences form inhibitory connections (Eq. 11). **(B)** The effective interaction for the connectivity in part A (Eq. 12).

Directional selectivity We have considered only neurons that are sensitive to one direction of motion of the stimulus (Fig. 2). Stimulating two clusters of neurons with co-linear bars moving in opposite directions, *i.e.*, $\Delta\theta_0 = 180°$, will not generate coherence between the activity of neurons in the two clusters.

It is known from experiment that even neurons that are not selective to the direction of motion exhibit oscillatory output in response to a stimulus moving either forward or backward (4,5). Yet the output of two such neurons remains uncorrelated when bars moving in opposite direction pass through their respective, receptive fields (4,5). These observations can be accounted for within the model by incorporating neurons that are insensitive to the direction of motion of the stimulus (Fig. 6). The short-range connections will not depend on the directional properties of the neurons. However, the long-range connections will occur predominantly between cells that are directionally selective and that have the *same* directional preference. As a consequence, only directionally sensitive neurons mediate the temporal coherence between different clusters. This leads to coherence between the output of neurons in separate clusters only when the two stimuli move in the same direction. In the remainder of the paper we will focus only on issues related to orientation selectivity. Thus we will assume for simplicity that all the neurons have directional sensitive tuning curves, as in Fig. 2.

Before presenting the results of our analysis of the model, we discuss the quantities that we wish to calculate.

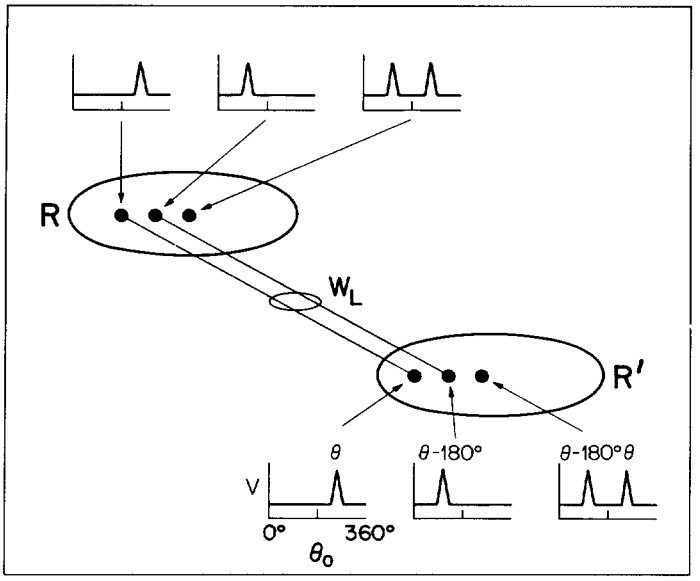

Figure 6. An architecture that incorporates neurons that are insensitive to the direction of motion of the stimulus as well as those that are sensitive to the direction.

Correlation functions

Coherent output in a population of neurons is deduced in experiment from the auto-correlogram of the output of each neuron and cross-correlograms of the output of pairs of neurons. The correlograms can be expressed in terms of the correlation functions of the underlying phase variables in the model. We define

$$\Phi_{\mathbf{R}}(\theta,t) = \omega t + \phi_{\mathbf{R}}(\theta,t) \tag{13}$$

where ϕ represents the noisy component of the total phase Φ for a neuron in the **R**-th cluster with orientation preference θ. The auto-correlogram is

$$<P_{\mathbf{R}}(\theta,t)\, P_{\mathbf{R}}(\theta,t+\tau)> = V_{\mathbf{R}}^2(\theta)\left(1 + \lambda^2 C_{\mathbf{R}}(\theta,\tau)\cos\omega\tau\right) \tag{14}$$

where $< \cdots >$ denotes averaging over time ($t >> 1/\omega$) and the auto-correlation function $C_{\mathbf{R}}(\theta,\tau) = <\cos(\phi_{\mathbf{R}}(\theta,t) - \phi_{\mathbf{R}}(\theta,t+\tau))>$ measures the temporal fluctuations in the phase.

The cross-correlogram of the activity of a neuron in the **R**-th cluster with orientation preference θ with one in the **R'**-th cluster with orientation preference θ' is

$$<P_{\mathbf{R}}(\theta,t)\, P_{\mathbf{R}'}(\theta',t+\tau)>_t = V_{\mathbf{R}}(\theta)V_{\mathbf{R}'}(\theta')\left(1 + \lambda^2 C_{\mathbf{R}\mathbf{R}'}(\theta,\theta',\tau)\cos\omega\tau\right) \tag{15}$$

where the cross-correlation function $C_{RR'}(\theta,\theta',\tau) = \langle\cos(\phi_R(\theta,t)-\phi_{R'}(\theta',t+\tau))\rangle$ measures the amplitude of the phase coherence. Synchronization occurs with zero phase-shift in our model; we return to this issue in the Discussion.

Results and Examples

The model was analyzed using mean-field theory (7,16) and applies when the number of active neurons in each cluster is large ($N \gg 1$). For concreteness, we assumed that the tuning curve for every neuron has the shape shown in Fig. 2. The main results are given below.

Temporal coherence within a single cluster. The presence of coherent oscillations depends on the rate of decay of the correlation functions. When the level of noise is large, the neurons behave as overdamped oscillators and both $C_R(\theta,\tau)$ and $C_{RR}(\theta,\theta',\tau)$ decay to zero in a time $\sim \tau_0/T \ll 1/\omega$ (dashed line; Fig. 7). In contrast, the neurons exhibit persistent, coherent oscillations when the level of noise is below a critical value, T_C, where

$$T_C = \frac{W_S}{2}\int_0^{2\pi}\frac{d\theta}{\sigma}\,V_R^2(\theta)\,. \tag{16}$$

For the tuning curve described by Eq. 3 (Fig. 2), $T_C = 0.5\ W_S$. When the noise level is less than T_C, the auto-correlation function decays from its initial value $C_R(\theta,0) = 1$ to a long-time limit $C_R(\theta) \equiv \lim_{\tau\to\infty} C_R(\theta,\tau) > 0$ (solid line; Fig. 7). This rapid decay is characterized by a time-constant

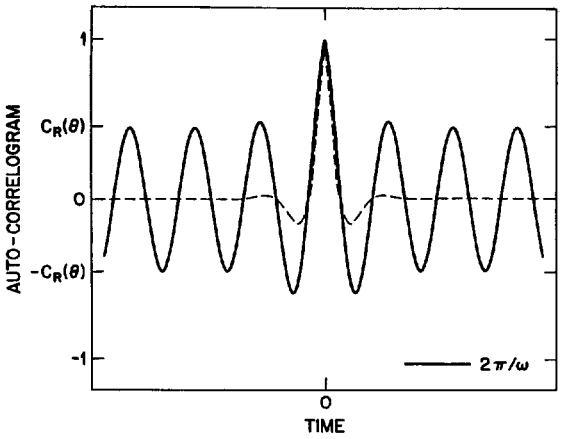

Figure 7. The time dependent part of the auto-correlogram for a neuron that is stimulated by a moving bar oriented at its preferred orientation, *i.e.*, $\theta = \theta_0$. We chose $W_S = 0.2$, for which $\tau_S \simeq 3\tau_0$ (Eq. 17) and $T_C = 0.1$ (Eq. 16) with $T = 0.2T_C$ (solid line) and $T = 5T_C$ (dashed line). The period of oscillations of the neurons was taken as $2\pi/\omega = 8\ \tau_0$.

$$\tau_S \simeq \frac{\tau_0}{2V_R(\theta)W_S} \tag{17}$$

and results in a peak in the auto-correlation function that is centered at $\tau = 0$ and has a width of $\sim 2\tau_S$. The magnitude of $C_R(\theta)$ depends on θ as well as the level of noise (Fig. 8). The presence of noise and the restricted number of active neurons in the cluster lead to an eventual decay of the correlation functions, characterized by a time-constant $\tau_L \sim N\tau_0/T >> 1/\omega$. Thus the long-time limit referred to above corresponds to $\tau_S << \tau << \tau_L$.

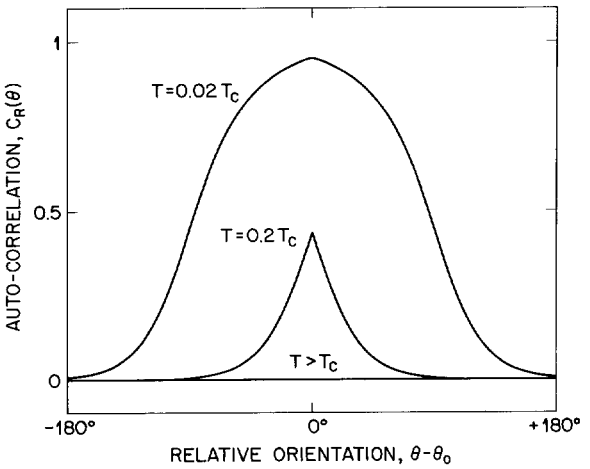

Figure 8. The dependence of the long-time limit of the auto-correlation function on the orientation of the stimulus relative to the preferred orientation of the neuron.

The cross-correlation functions between neurons in the same cluster do not have a substantial peak centered at $\tau = 0$. Their magnitude is related to the long-time limit of their auto-correlation functions through

$$C_{RR}(\theta,\theta',\tau) = \sqrt{C_R(\theta)\ C_R(\theta')}\ . \tag{18}$$

There are no phase-shifts associated with the cross-correlation, *i.e.*, $\chi = 0$ (Eq. 15), as the short-range connections are excitatory. Thus, all of the active neurons in a cluster will fire coherently as a result of the extensive, short-range connectivity.

Temporal coherence of spatially separated clusters. The coherence between neurons that belong to two separate clusters depends on the coherence of the *average* phases

of the clusters. The cross-correlation function between a neuron in the **R**-th cluster with one in the **R'**-th cluster is

$$C_{\mathbf{RR'}}(\theta,\theta',\tau) = \sqrt{C_{\mathbf{R}}(\theta)\, C_{\mathbf{R'}}(\theta')}\; C_{\mathbf{RR'}} \tag{19}$$

where $C_{\mathbf{RR'}}$ measures the correlation of the average phases of the two clusters for times $\tau \ll N\tau_0 \sim \tau_L$.

The extent of the coherence between active clusters depends on their direct interaction as well as indirect interactions via other active clusters. We consider below several examples of extended stimuli and demonstrate the dependence of $C_{\mathbf{RR'}}$ (Eq. 19) on global features of the stimulus. For each example we use the form of $F(\theta-\theta')$ given by Eq. 11 (Fig. 4A), with ϵ chosen so that the half-width at half-maximum of $J_{\mathbf{RR'}}$ is half that of the tuning curve.

Stimulation by two short bars. The simplest example of long-range coherence involves two clusters that are stimulated by separate, short bars whose length spans the individual receptive fields. The correlation of the average phases of the two clusters depends on the *relative* orientation of the bars through $J_{\mathbf{RR'}}$ (solid lines, Fig. 9). Note that the choice $F(\theta-\theta') = \sigma\,\delta(\theta - \theta')$ (Eq. 9) results in a relatively weak dependence of $C_{\mathbf{RR'}}$ on $\Delta\theta_0$ (dashed line, Fig. 9).

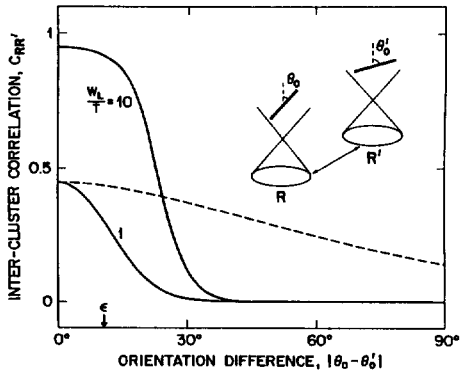

Figure 9. The correlation between the average phases of two clusters as a function of the difference in orientation of two moving, short bar. The solid lines were calculated with $F(\theta - \theta')$ including excitatory as well as inhibitory connections (Eq. 11) while the dashed lines refer to purely excitatory connections (Eq. 9).

Short versus long bars. The coherence between clusters can be enhanced when several receptive fields, as opposed to just two fields, are stimulated by bars moving with the same orientation. The enhancement depends on the magnitude of W_L/T and is most pronounced when this ratio is smaller than unity (Fig. 10). The experimental evidence (4) is consistent with $W_L/T \lesssim 1$.

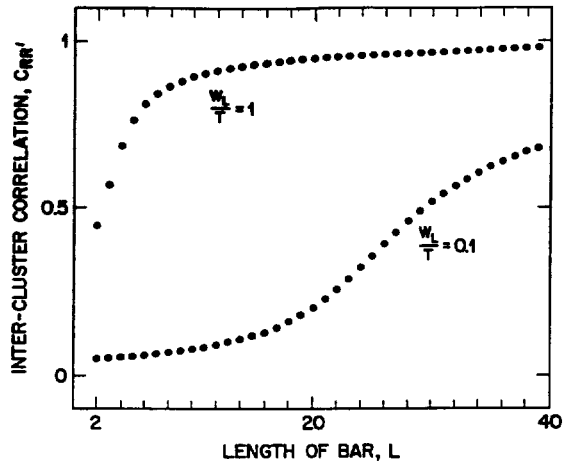

Figure 10. The enchancement in the correlation between two spatially separated clusters that are stimulated by a moving, long bar as opposed to two co-linear, short bars. The length of the bar, L, is expressed as the number of receptive fields that it spans.

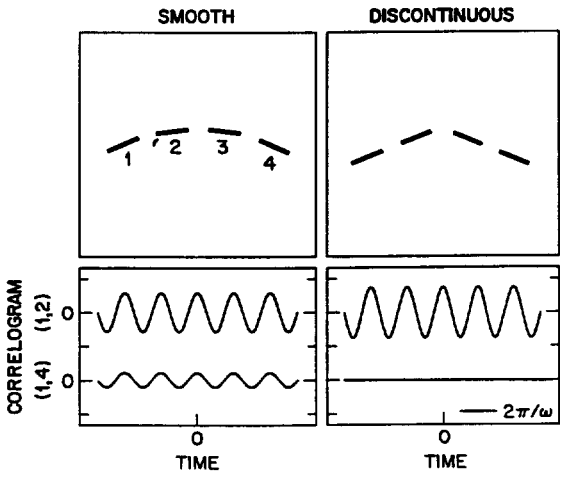

Figure 11. Segmentation of four oriented bars that span several receptive fields. The bars are of equal length and spacing and are arranged to subtend the same total angle ($W_L/T = 1$ and $L = 5$). **(A)** Bars arranged as a smoothly varying stimulus. **(B)** Bars arranged as discontinuous stimuli. **(C)** The pair-wise correlations between adjacent clusters are equal; $C_{12} = C_{23} = C_{34} \simeq 0.6$ ($\Delta\theta_0 = 15°$). Neurons in all of the active clusters fire coherently and the end-to-end correlation is $C_{14} = (C_{12})^3 \simeq 0.2$. **(D)** The pair-wise correlations between adjacent clusters are $C_{12} = C_{34} \simeq 0.8$ ($\Delta\theta_0 = 0°$) and $C_{23} \simeq 0$ ($\Delta\theta^0 = 45°$). The end-to-end correlation is $C_{14} \simeq 0$.

Extended curved objects. The curvature of stimuli that span several receptive fields can be used to segment a stimulus into separate objects. We illustrate this by considering the coherence between clusters in the presence of four, long bars with orientations that vary in space (Fig. 11). In the case of a smooth variation there is a substantial correlation between the output of neurons in all pairs of clusters, including those at the end of the object. In contrast, with a discontinuous variation in orientation the coherent activity of the neurons is segmented into two groups.

Discussion

We used a phenomenological model that greatly simplified the neuronal dynamics. The advantage of this approach is that the description of the temporal and spatial coherence in the neurons involves few parameters, *e.g.*, the scales of short-range and long-range connection strength and the level of noise. These parameters can, in principle, be determined from the amplitude and time-dependence of the measured correlation functions. Further, there are predicted relationships among the correlation functions (Eqs. 18 and 19). The experimental determination of these scales and relationships will test the consistency of the model.

Architecture of connectivity. Our model assumed that neurons that share the same receptive field are grouped in clusters. The interactions between neurons within a clusters are strong and depend only moderately on the orientation preference of the neurons. The interactions between neurons in different clusters are relatively weak and depend strongly on their orientation preference.

This architecture offers a number of attractive computational features, some of which have been alluded to above (Figs. 9-11). Quite generally, this architecture allows proximal stimuli with disparate features to be linked as a single object. Consider, for example, the recognition of the connected versus the disconnected pattern in Fig. 12. For the connected pattern, the neurons that respond to orthogonal segments interact via short-range connections. Thus all of the neurons oscillate coherently. For the disconnected pattern, the neurons that respond to orthogonal segments do not interact. Thus their output is segmented into two coherent populations. In addition, the architecture in our model may provide a mechanism for linking several features, *e.g.*, orientation and color, that are processed by different neurons that share the same receptive field.

The notion that the specificity of cortical connections depends on the orientation preference of cells is supported by physiological and anatomical data (17,18). The majority of the evidence indicates that there are excitatory interactions between cells with similar preferences. Further, there are claims of inhibitory interactions between cells with different orientation preferences (19,20).

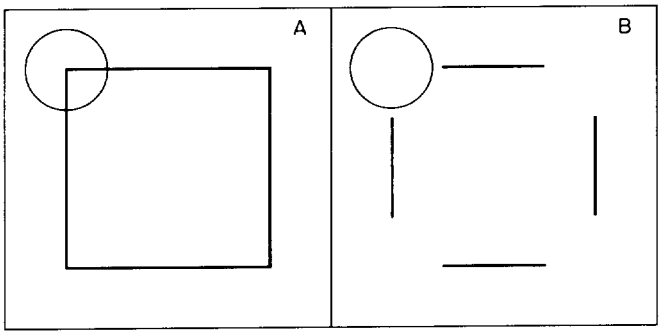

Figure 12. Patterns formed from orthogonal lines. (A) A continuous pattern. (B) A discontinuous pattern. The circles correspond to the assumed upper bound on the size of a receptive field. Within the framework of our model, the neurons that respond to the continuous pattern are fully synchronized, while those that respond to the discontinuous object are segmented into two populations.

The relative non-specificity of the short-range interaction assumed in our model is supported by the relative insensitivity of the coherence of proximal neurons to their orientational preference (2,4). However, other physiological data on orientation specificity of connections does not reveal a clear difference between short-range and long-range connections (17,21). Further, there are recent indications that the coherence of the oscillations of proximal neurons, stimulated by two moving bars, is sensitive to the relative orientation of the bars (22). This important issue deserves further experimental and theoretical study.

Activity dependence of the connections. The interaction between the phases of the pre-synaptic and post-synaptic neurons depends on their level of activity (Eq. 5). This form is suggestive of a fast Hebb-like modification of the strength of synaptic connections. A *possible* biophysical basis for these fast changes are excitatory synaptic currents that are mediated by N-methyl-D-aspartate (NMDA) receptors (23). Indeed, there are recent experimental findings that suggest that NMDA receptors mediate a significant fraction of the synaptic currents in the primary visual cortex (24).

Activity dependent couplings between phases may also emerge as a consequence of the interactions among neuronal oscillators in which both amplitudes and phases are dynamic variables. In such a network, the couplings between the phase of the neuronal oscillations will depend on activity of the neurons even when the underlying synaptic interactions have a fixed strength. This dynamic effect may, in principle, account for the required dependence of the phase coherence on the activity of the pre- and post-synaptic cell. A preliminary analysis of this effect was performed by considering a network of analog neurons. The neurons in each receptive field were arranged as two populations, one that formed exclusively excitatory connections and the other that formed exclusively inhibitory connections (25). The neurons

in the excitatory population received an external input whose magnitude depended on the orientation preference of the cell relative to the orientation of the stimulus, *i.e.*, $I = I(\theta_0 - \theta)$. Such a network exhibits oscillatory output as a cooperative phenomena for an appropriate range of parameters (25).

Two such networks, representing two clusters, were coupled via a set of weak, excitatory connections with fixed strength. The connections were formed only between neurons with the same orientation preference (Eq. 9). The correlation function between the output of the two clusters, $C_{\mathbf{R}\mathbf{R}'}$, calculated by numerical simulation, showed a strong dependence on the orientation difference $|\theta_0 - \theta_0'|$ (unpublished results with E. Grannan). This dependence was substantially greater than the relatively poor discrimination observed in the phase model with Hebb-like connections (Eq. 5) between neurons with the same orientation preference (Eq. 9) (dashed line, Fig. 9). These results suggest that the activity-dependent interactions between the phases of neurons may be a dynamic effect. Further, the dependence on the activity that is induced by the dynamics appears to be highly non-linear and may lead to strong discrimination even without feature specific, inhibitory long-range connections.

Time-delays and phase-shifts. We have assumed that the interactions between phases are predominantly positive and have zero time-delays. Thus the absence of phase-shifts is expected. However, the local connections between cortical neurons are mediated by unmyelinated axons with slow propagation speeds, *i.e.*, $\sim$ 1 mm/ms (17). It is thus important to consider the possible effect of time delays on the synchronization of oscillations and, in particular, on the phase-shifts between the output of different neurons.

The propagation time for distances of $\sim$ 1 mm is $\sim$ 1 ms, which is much smaller than the period of the oscillations, $2\pi/\omega = 25$ ms. Thus the delays are not expected to affect the synchronization within a cluster. On the other hand, the propagation delays between synchronized neurons that are 7 - 10 mm apart cannot be ignored. To study the effect of the delays in the long-range connections, we have considered (18) the synchronization of two active clusters described by phase equations with delayed interactions, *i.e.*,

$$\tau_0 \dot{\Psi}_{\mathbf{R}}(t) = \tau_0 \omega_0 - J_{\mathbf{R}\mathbf{R}'} \sin\left(\Psi_{\mathbf{R}}(t) - \Psi_{\mathbf{R}'}(t - \tau_D)\right)$$

$$\tau_0 \dot{\Psi}_{\mathbf{R}'}(t) = \tau_0 \omega_0 - J_{\mathbf{R}\mathbf{R}'} \sin\left(\Psi_{\mathbf{R}'}(t) - \Psi_{\mathbf{R}}(t - \tau_D)\right) \qquad (20)$$

where $\Psi_{\mathbf{R}}$ and $\Psi_{\mathbf{R}'}$ are the average phases of the clusters at locations $\mathbf{R}$ and $\mathbf{R}'$, respectively, τ_D represents the average propagation delay between pairs of neurons in the two clusters and we have neglected noise. This model is similar to that studied by Schuster and Wagner (26).

An analysis similar to that in ref. (26) shows that there are periodic solutions of Eq. 20 with a frequency, $\omega \neq \omega_0$, that depends on the value of $J_{RR'}$ and τ_D. The phase-shift between the two oscillators is either 0 or π. Periodic solutions with zero phase-shifts are stable if

$$0 < \tau_D < \frac{\pi}{2\omega} \tag{21}$$

It is important to note that the bounds on τ_D are in terms of the true frequency of the system, ω, and not in terms of the driving frequency, ω_0. For the oscillations in the visual cortex, this result implies that the synchronization of the neurons is not disrupted for $\tau_D \lesssim 6$ ms. This bound corresponds to a propagation delay between neurons that separated by roughly 5 mm.

The role of noise. The presence of noise plays a vital role in controlling the coherence throughout the network. This is particularly crucial for dephasing the output of only weakly interacting clusters. Random variation in the driving frequency of each neuron ($\omega(\mathbf{r})$; Eq. 4) is an additional, potential source of noise. Networks of coupled oscillators with a distribution of driving frequencies will remain coherently active provided that the width of this distribution is small relative to the strength of the interactions within a cluster (15), *i.e.*, $|\delta\omega| \lesssim 1/\tau_S$ (Eq. 17). In general, the coherence between difference clusters can also be modulated by a variation of the driving frequency with some property of the stimulus. Systematic variation of the frequency with the velocity of visual stimuli is observed (2,5).

This work was supported, in part, by the Fund for Basic Research administered by the Israeli Academy of Arts and Sciences and by the US-Israel Binational Science Foundation. D. G. thanks AT&T Bell Laboratories for its hospitality.

References

1. von der Malsburg, C. & Schneider, W. (1986) A neural cocktail-party processor. *Biol. Cybern.* **54,** 29-40.
2. Eckhorn, R., Bauer, R., Jordan, W., Brosch, M., Kruse, W., Munk, M. & Reitboek, R. J. (1988) Coherent oscillations: A mechanism of feature linking in the visual cortex. Multiple electrode and correlation analysis in the cat. *Biol. Cybern.* **60,** 121-130.
3. Gray, C. M. & Singer, W. (1989) Stimulus-specific neuronal oscillations in orientation columns of cat visual cortex. *Proc. Natl. Acad. Sci. USA* **86,** 1698-1702.
4. Gray, C. M., Konig, P., Engel, A. K. & Singer, W. (1989) Oscillatory responses in cat visual cortex exhibit inter-columnar synchronization which reflects global stimulus properties. *Nature* **338,** 334-337.
5. Gray, C. M., Engel, A. K., Konig, P., & Singer, W. (1990) Stimulus-dependent neuronal oscillations in cat visual cortex I. Receptive field properties and feature dependence. *Eur. J. Neurosci.*, in press.
6. Engel, A. K., Konig, P., Gray, C. M., & Singer, W. (1990) Stimulus-dependent neuronal oscillations in cat visual cortex II. Inter-columnar interactions as determined by cross-correlation analysis. *Eur. J. Neurosci.*, in press.
7. Sompolinsky, H., Golomb, D. & Kleinfeld, D. (1990) Global processing of visual stimuli in a neural network of coupled oscillators. *Proc. Natl. Acad. Sci. USA* ,in press.
8. Spourns, O., Gally., J. A., Reeke, G. N. & Edelman, G. M. (1989) Reentrant signaling among simulated neuronal groups leads to coherency in their oscillatory activity. *Proc. Natl. Acad. Sci. USA* **86,** 7265-7269.

9. Kammen, D. M., Holmes, P. J. & Koch, C. (1989) Cortical architecture and oscillations in neuronal networks: Feedback versus local coupling. In *Models of Brain Function*, ed. Cotterill, R. M. J. (Chambridge University Press, UK), pp. 273-284.

10. Eckhorn, R., Reitboeck, R. J., Dicke, P., Arndt, M. & Kruse, W. (1990) Feature linking across cortical maps via synchronization. In *Parallel Processing in Neural Systems and Computers*, eds. Eckmiller, R., Hartman, E. & Hauske, G. (Elsevier Science Publishers, Holland), pp. 101-104.

11. Schillen, T. B. & Konig, P. (1990) Coherency detection by coupled oscillatory responses: Synchronizing connections in neural oscillator layers. In *Parallel Processing in Neural Systems and Computers*, eds. Eckmiller, R., Hartman, E. & Hauske, G. (Elsevier Science Publishers, Holland), pp. 139-142.

12. Schuster, H. G. & Wagner, P. (1990) A model for neuronal oscillations in the visual cortex. In *Parallel Processing in Neural Systems and Computers*, eds. Eckmiller, R., Hartman, E. & Hauske, G. (Elsevier Science Publishers, Holland), pp. 143-146.

13. Wilson, M. A. & Bower, J. M. (1990) Computer simulation of oscillatory behavior in cerebral cortical networks. In *Advances in Neural Network Information Processing Systems 2*, ed., Touretzky, D. (Morgan Kaufmann Publishers, Inc., CA).

14. Lytton, W. & Sejnowski, T. (1990) Inhibitory interneurons may help synchronize oscillations in cortical pyramidal neurons. Submitted.

15. Kuramoto, Y. (1984) *Chemical Oscillations, Waves, and Turbulence* (Springer-Verlag, NY).

16. Sompolinsky, H., Golomb, D. & Kleinfeld, D. (1990) Cooperative dynamics in visual processing. *Phys. Rev. A*, to be submitted.

17. Gilbert, C. D. (1983) Microcircuitry of the visual cortex. *Ann. Rev. Neurosci.* **6**, 217-247.

18. Martin, K. A. C. (1984) Neuronal circuits in cat striate cortex. In *Cerebral Cortex, Vol. 3*, eds. Jones, E. G. & Peters, A. (Plenum Press, NY), pp. 241-284.

19. Matsubara, J. A., Cynader, M. S. & Swindale, N. V. (1987) Anatomical properties and physiological correlates of the intrinsic connections in cat area 18. *J. Neurosci.* **7**, 1428-1446.

20. Hata, Y., Tsumoto, T., Hagihara, K & Tamura, H. (1988) Inhibition contributes to orientation selectivity in visual cortex of cat. *Nature* **335**, 815-817.

21. Ts'o, D. Y., Gilbert, C. D. & Wiesel, T. N. (1986) Relationships between horizontal interactions and functional architecture in cat striate cortex as revealed by cross correlation analysis. *J. Neurosci.* **6**, 1160-1170.

22. Engel. A. K., Konig, P., Gray, C. M. & Singer, W. (1990) Synchronization of oscillatory responses: A mechanism for stimulus-dependent assembly formation in cat visual cortex. In *Parallel Processing in Neural Systems and Computers*, eds. Eckmiller, R., Hartman, E. & Hauske, G. (Elsevier Science Publishers, Holland), pp. 105-108.

23. Gray, C. M., Konig, P., Engel, A. K. & Singer, W. (1990) Synchronization of oscillatory responses in visual cortex: A plausible mechanism for scene segmentation. In *Synergetics of Cognition*, eds., Haken, H. & Stadler, M. (Springer-Verlag, NY) pp. 82-98.

24. Miller, K. D., Chapman, B. & Stryker, M. P. (1989) Visual responses in adult cat visual cortex depend on N-methyl-D-aspartate receptors. *Proc. Natl. Acad. Sci. USA* **86**, 5183-5187.

25. Sompolinsky, H. (1988) Statistical mechanics of neural networks. *Physics Today* **41**, 40-80.

26. Schuster, H. G. & Wagner, P. (1989) Mutual entrainment of two limit cycle oscillators with time delayed coupling. *Prog. Theor. Phys.* **81**, 939-945.

27. Orban, G. A. (1984) *Neuronal Operations in the Visual Cortex* (Springer-Verlag, NY).